Wavepaths in inhomogeneous media

Marta Jo Woodward

ABSTRACT

The Rytov wavepath examples of SEP–57 (Woodward, 1988) are extended from homogeneous to inhomogeneous background media. The wavepaths are constructed from monochromatic Green's functions, calculated by Fourier transformation over time of data cubes ($d(x,z,t)$) generated by finite-difference modelling.

INTRODUCTION

In SEP–57, Rytov wave-equation tomography was formulated in a fashion parallel to ray-trace tomography (Woodward, 1988). Scattered phases were shown to be projected back over monochromatic, source-receiver *wavepaths* in the former, just as traveltime delays are projected back over infinite-bandwidth, source-receiver *raypaths* in the latter. Monochromatic wavepaths were identified as products between source- and receiver-centered Green's functions, derived for the background medium:

$$\mathcal{L}(\mathbf{x}|\mathbf{s},\omega) = 2k_0^2 \frac{G_0(\mathbf{r}-\mathbf{x}|\omega)G_0(\mathbf{s}-\mathbf{x}|\omega)}{G_0(\mathbf{s}-\mathbf{r}|\omega)}. \tag{1}$$

(Here $\mathbf{s}$, $\mathbf{r}$, and $\mathbf{x}$ are source, receiver, and space coordinates, respectively; ω is frequency; k_0 is the background wavenumber).

The examples in SEP–57 were confined to homogeneous background media, where wavepaths are easily constructed from analytic expressions for free-space Green's functions. For inhomogeneous background media, explicit solutions for Green's functions are not always available. When the background medium varies slowly on the scale of the source wavelength, Green's functions can be obtained numerically, by application of the WKBJ approximation and solution of the eikonal and transport equations (Clayton and Stolt, 1981; Miller et al., 1987). Given a fast computer, a more general method for finding Green's functions is the Fourier transformation over time of data cubes, $d(x,z,t)$, generated by finite-difference

modelling. Each frequency slice through the transformed cube, $D(x,z,\omega)$, is a monochromatic Green's function.

Following are three examples of monochromatic Green's functions and Rytov wavepaths (normalized by k_0^2) for one-dimensional, inhomogeneous media. The figures were calculated using a two-dimensional, acoustic, finite-difference program. Inspection of the pictures clarifies the connection between raypaths and wavepaths, and consequently the relation between ray-trace and wave-equation tomography.

REFRACTION THROUGH A VERTICAL GRADIENT

Figure 1 shows a 15 Hz Green's function and wavepath (imaginary parts and moduli) for a source and receiver positioned above a vertical velocity gradient. The model is 8000 m by 4990 m; the velocity increases linearly from 1007 m/s to 6000 m/s. The low frequency artifacts at the bottoms and sides of the panels result from imperfect absorbing boundaries. The wavepath is clearly refracted along the circular path predicted by ray theory (Dobrin, 1976). Integration of wavepaths over frequency would yield the familiar, infinite-bandwidth raypath (Woodward, op. cit.).

REFLECTION ABOVE AN INTERFACE

Figure 2 shows a 15 Hz Green's function and wavepath (imaginary parts and moduli) for a source and receiver positioned above a velocity interface. The model is 8000 m by 4990 m; the upper and lower velocity layers are 2000 m/s and 3620 m/s, respectively. The Green's function has several interesting features: null zones appear both where the direct and reflected wavefields interfere, and beneath the interface, beyond the critical angle; the critical reflection emerges as a high amplitude feature, perhaps reinforced by the head wave.

The wavepath contains two elliptical features: a horizontal ellipse describing the direct arrival, and a folded ellipse describing the post-critical, reflection arrival. The weaker, head-wave arrival is not readily apparent. Unlike the previous (or following) example, the interior regions of the ellipses change sign from frequency to frequency, as determined by interference between the direct, reflected and refracted events. For this experiment, integration of wavepaths over frequency would not produce a raypath equivalent. This breakdown in the parallelism between Rytov and ray-trace tomography occurs when multiple background arrivals are considered simultaneously; phase unwrapping becomes impossible, and the Rytov approximation's transmission-tomography advantage over the Born approximation disappears (Keller, 1969; Beydoun and Tarantola, 1987). The problem can be remedied by distinguishing background arrivals with windowing, and by artificially constructing single-path wavepaths.

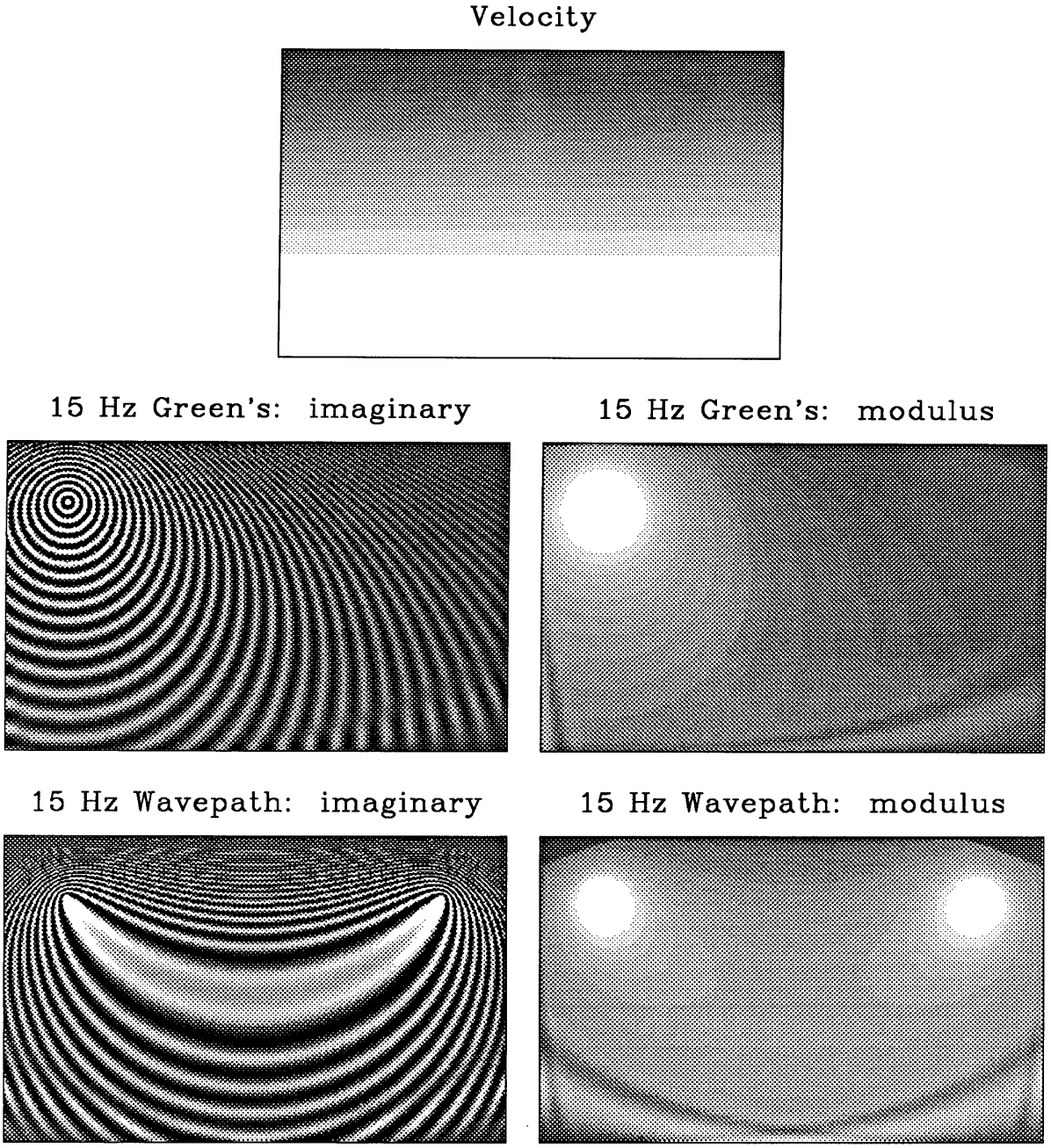

FIG. 1. 15 Hz Green's function and wavepath (imaginary parts and moduli) for a refraction experiment through a vertical velocity gradient. The wavepath of equation 1 has been normalized by k_0^2.

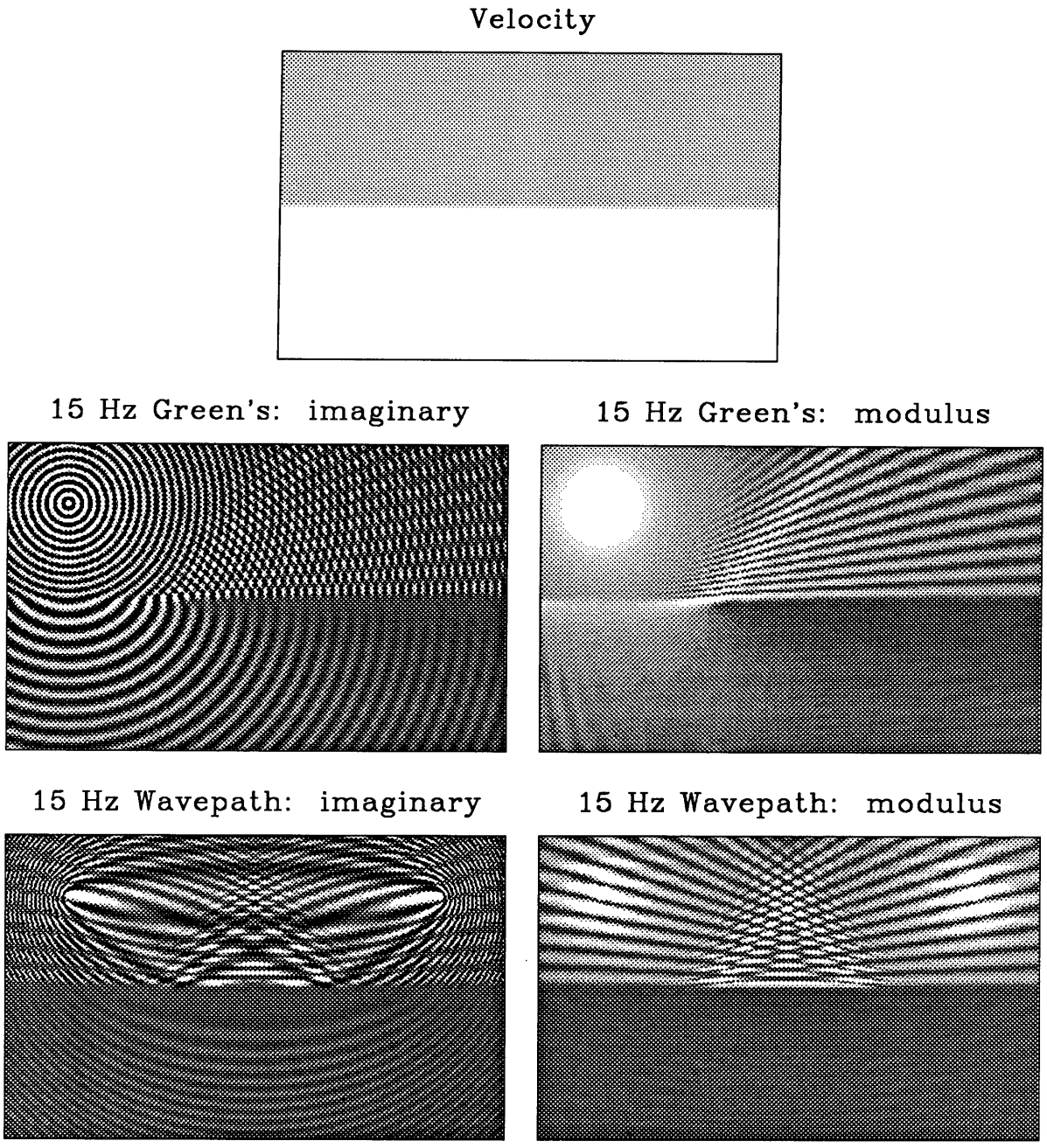

FIG. 2. 15 Hz Green's function and wavepath (imaginary parts and moduli) for a transmission and reflection experiment above a velocity interface. The wavepath of equation 1 has been normalized by k_0^2.

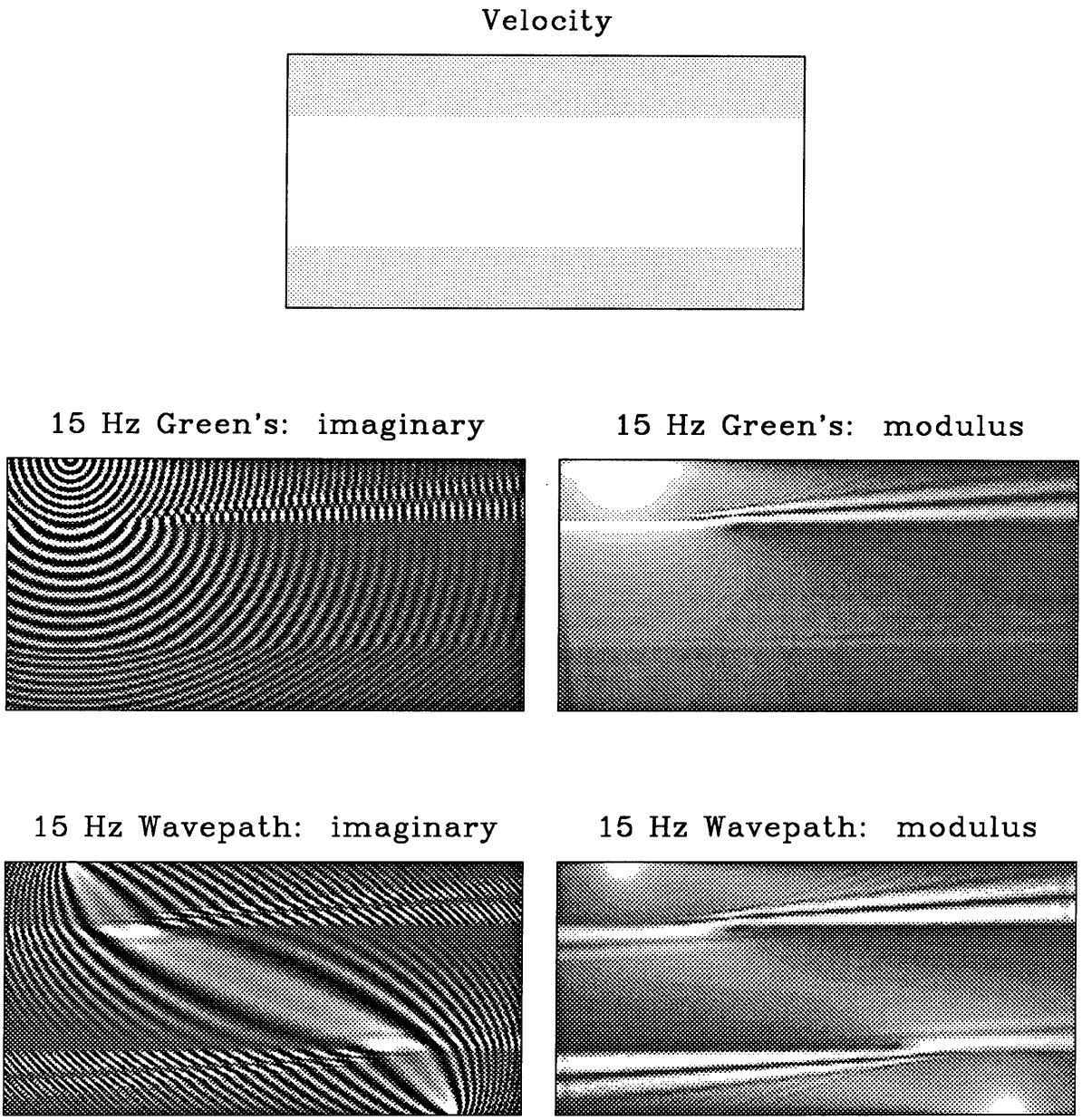

FIG. 3. 15 Hz Green's function and wavepath (imaginary parts and moduli) for a transmission experiment through three velocity layers. The wavepath of equation 1 has been normalized by k_0^2.

TRANSMISSION THROUGH LAYERS

Figure 3 shows a 15 Hz Green's function and wavepath (imaginary parts and moduli) for a transmission experiment, with source and receiver positioned on opposite sides of three velocity layers. The model is 8000 m by 4000 m; a 3000 m/s layer lies between two 2000 m/s layers. The wavepath is refracted along the bent path predicted by ray theory.

CONCLUSION

Wavepaths provide a tool for visualizing the sampling of a velocity field by a source-receiver experiment. The Rytov wavepath predicts the sensitivity of the recorded wavefield to the presence of an anomaly in the background medium. The single-arrival experiments of Figures 1 and 3 emphasize the similarity between wavepaths and raypaths as forward modelling and backprojection operators. The multiple-arrival experiment of Figure 2 points out the reliance of Rytov, transmission tomography on the separation of background events.

ACKNOWLEDGEMENTS

John Etgen's acoustic, finite-difference program produced the synthetic wavefields examined in this paper. Francis Muir suggested the example of Figure 1.

BIBLIOGRAPHY

Beydoun, W. B., and Tarantola, A., 1987, First Born and Rytov approximations: modeling and inversion conditions in a canonical example: Submitted to The Journal of the Acoustical Society of America.

Dobrin, M. B., 1976, Introduction to Geophysical Prospecting: McGraw-Hill, 310.

Clayton, R. W., and Stolt, R. H., 1981, A Born-WKBJ inversion method for acoustic reflection data: Geophysics, **46**, 1559–1567.

Keller, J. B., 1969, Accuracy and validity of the Born and Rytov approximations: J. Opt. Soc. Am., **59**, 1003–1004.

Miller, D., Oristaglio, M., and Beylkin, G., 1987, A new slant on seismic imaging: Migration and integral geometry: Geophysics, **52**, 943–964.

Woodward, M. J., 1987, Wave-equation tomography I: SEP–**57**, 1–23.